Supplementary material: Tensile and compressive stresses in Cu/W multilayers: correlation with microstructure, thermal stability, and thermal conductivity

Giacomo Lorenzin, Md Shafkat Bin Hoque, Daniel Ariosa, Lars P.H. Jeurgens, Eric R. Hoglund, John A. Tomko, Patrick E. Hopkins, and Claudia Cancellieri

Giacomo Lorenzin, Lars P.H. Jeurgens, and Claudia Cancellieri*
Empa, Swiss Federal Laboratories for Materials Science and Technology, Laboratory for Joining Technologies and Corrosion, Überlandstrasse 129, 8600 Dübendorf, Switzerland.

Md Shafkat Bin Hoque and John A. Tomko
Department of Mechanical and Aerospace Engineering, University of Virginia, Charlottesville, VA, 22904

Daniel Ariosa
Instituto de Física, Facultad de Ingeniería, Universidad de la República, Herrera y Reissig 565, C.C. 30, Montevideo 11000, Uruguay

Eric R. Hoglund
Department of Materials Science and Engineering, University of Virginia, Charlottesville, Virginia 22904, USA

Patrick E. Hopkins
Department of Mechanical and Aerospace Engineering, University of Virginia, Charlottesville, Virginia 22904, USA
Department of Materials Science and Engineering, University of Virginia, Charlottesville, Virginia 22904, USA and
Department of Physics, University of Virginia, Charlottesville, Virginia 22904, USA

(Giacomo Lorenzin and Md Shafkat Bin Hoque contributed equally to this work)

(Dated: August 4, 2022)

I. SPUTTERING CHAMBER AND MULTI-BEAM OPTICAL STRESS SENSOR

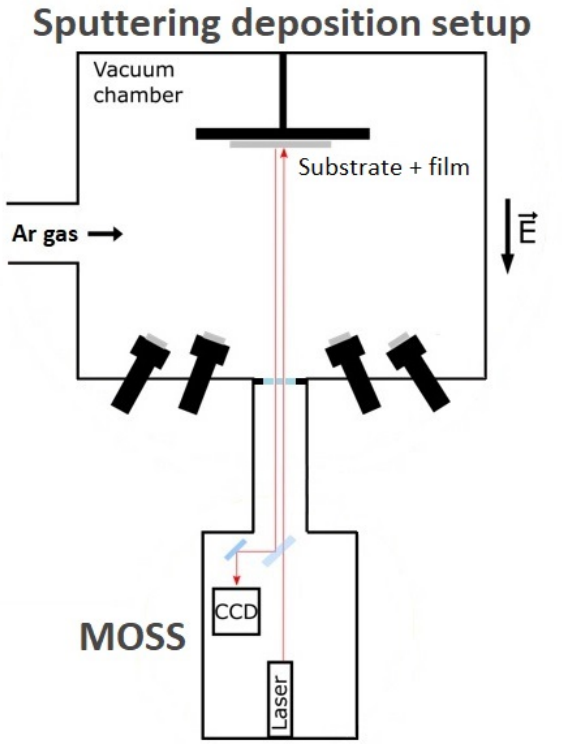

FIG. S1: Sputtering deposition chamber equipped with a Multi-beam Optical Stress Sensor (MOSS).

* claudia.cancellieri@empa.ch

II. SPUTTERING CHAMBER AND XPS

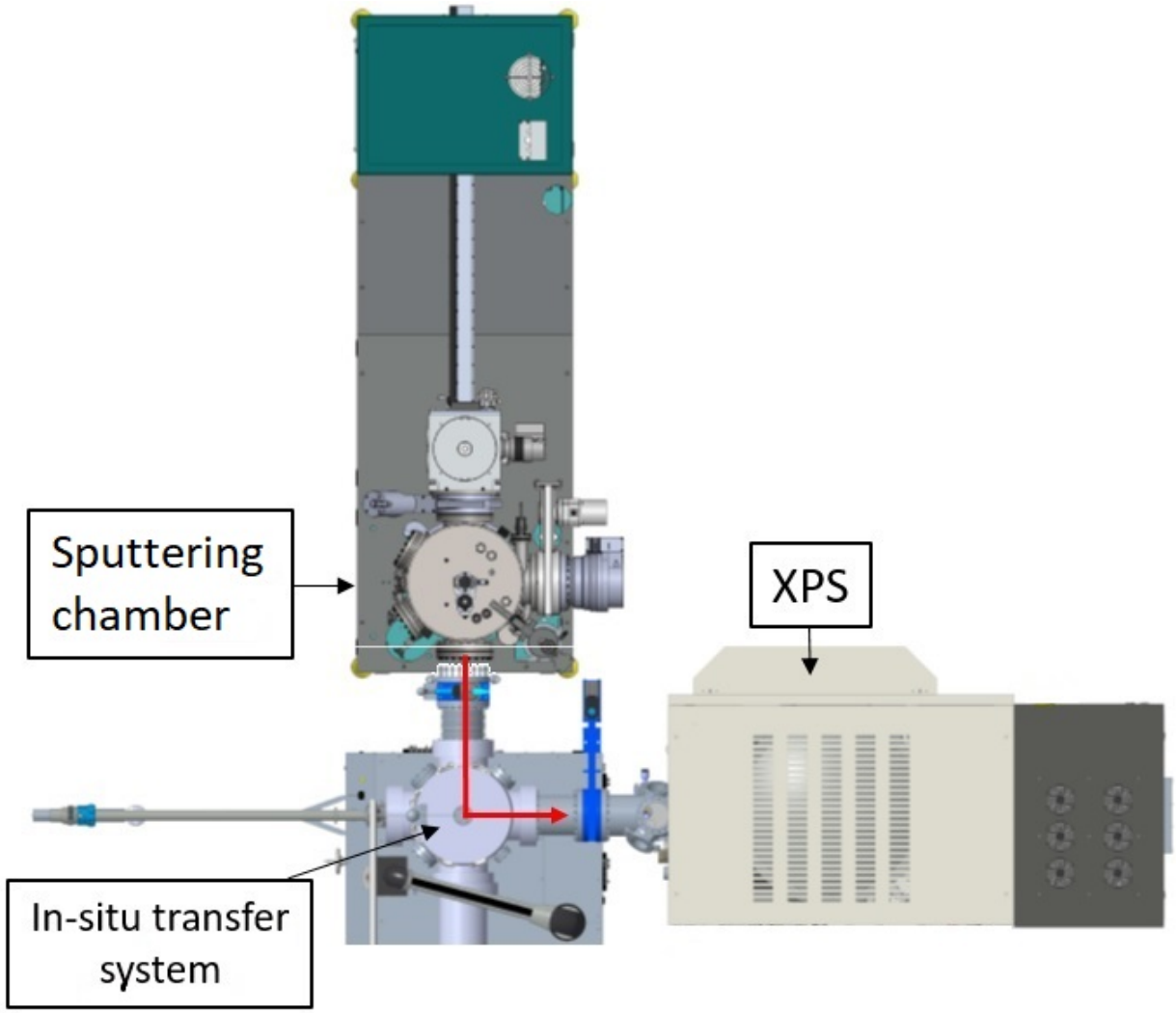

FIG. S2: View from the top of the sputtering chamber and the XPS. They are connected by a transfer system which allows the transfer of an as-deposited multilayer from the deposition chamber to the XPS without exposing it to air (red arrow).

III. TEXTURE

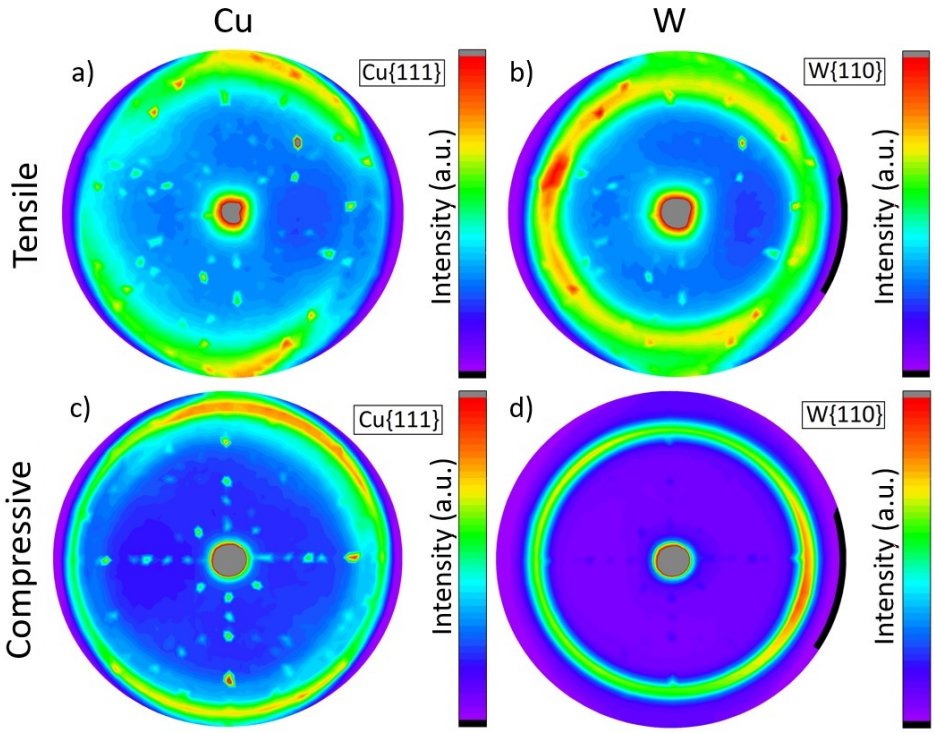

FIG. S3: Pole figures of Cu $\{111\}$ and W$\{110\}$ for tensile (a), (b) and compressive (c), (d) NMLs, respectively. Both in the tensile and in the compressive NMLs, Cu and W exhibit $\{111\}$ and $\{110\}$ fiber textures, respectively. However, the angular spreading is less pronounced in the compressive sample, suggesting a more ordered structure compared to the tensile sample.

IV. SEM IMAGES OF THE SURFACE OF AS DEPOSITED SAMPLES

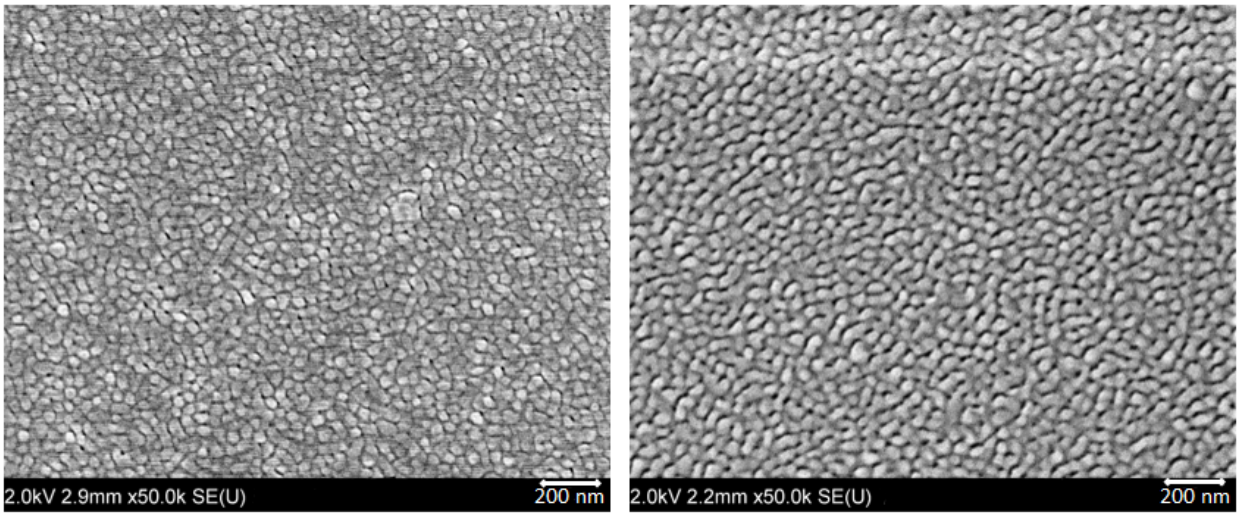

FIG. S4: SEM images of the surfaces of a Cu/W NML (a) tensile and (b) compressive, both as deposited.

V. MICROSTRUCTURE RESULTS AFTER ANNEALING

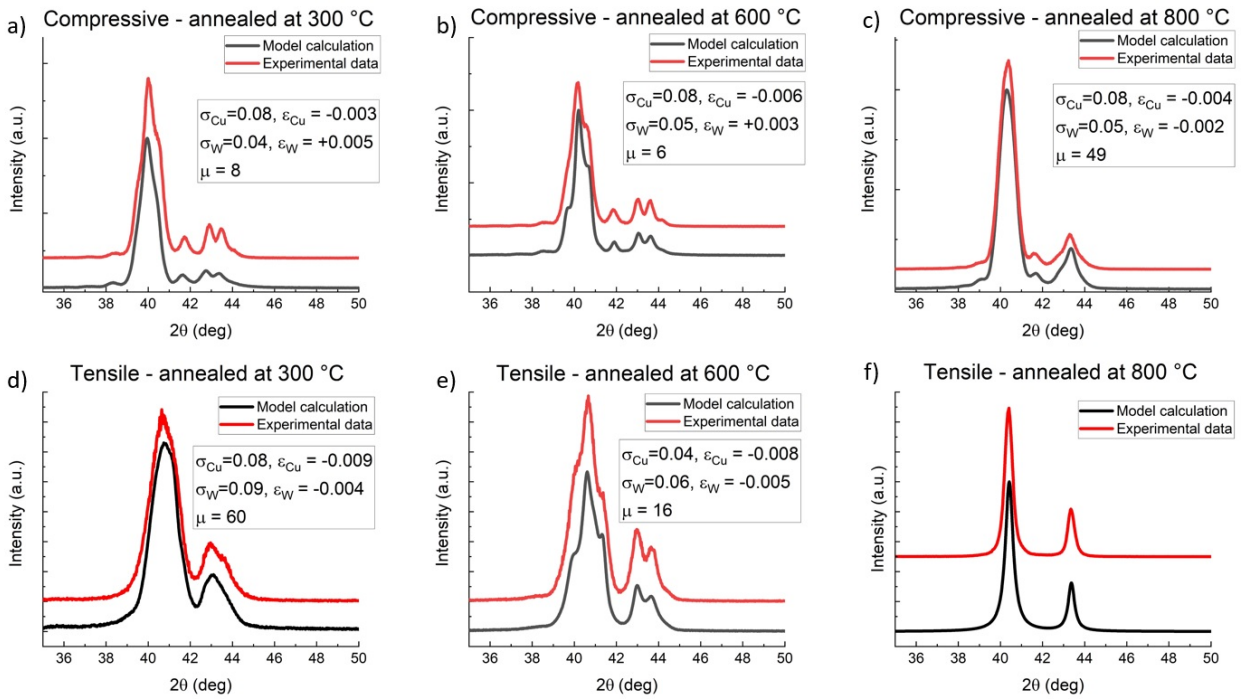

FIG. S5: XRD simulations for compressive Cu/W NML annealed at (a) 300 °C, (b) 600 °C and (c) 800 °C and tensile Cu/W NML annealed at (d) 300 °C, (e) 600 °C and (f) 800 °C. The simulation parameters are also indicated.